

## Chapter 3

# Simulations in the San Francisco Area

This chapter presents the responses of twenty-story, steel moment-resisting frame (MRF) buildings to simulated earthquakes in the San Francisco Bay area. Aagaard et al. (2008a,b) generated scenario ground motions for the 1989 Loma Prieta and 1906 San Francisco earthquakes, as well as two magnitude 7.8 ruptures on the northern San Andreas fault. I apply these long-period ground motions to two models of twenty-story buildings, and I compare the response of the stiffer, higher-strength building to that of the more flexible, lower-strength building. I also compare the responses of buildings modeled with fracture-prone welds to the responses of buildings with sound welds.

The 1989 magnitude 6.9 Loma Prieta and 1906 magnitude 7.9 San Francisco scenario earthquakes also demonstrate how much more damaging a great earthquake can be compared to a moderate or large earthquake. The seismic response of steel MRF buildings would be significantly different in repeats of each historic earthquake. The areal extent of inelastic building responses in the 1989 Loma Prieta scenario is tiny compared to that in the 1906 San Francisco scenario. Steel MRF buildings in the entire San Francisco Bay region would be affected by a magnitude 7.8 earthquake on the northern San Andreas fault segment near San Francisco. A magnitude 6.9 earthquake would affect a more limited region.

### 3.1 Ground Motion Study

Several researchers generated ground motions of the 1906 San Francisco earthquake on the occasion of its centennial anniversary (Aagaard et al., 2008a,b). The researchers employed new models of the geologic structure and seismic wave speeds in the San Francisco region. To validate their methods and models, the researchers simulated scenario ground motions for the 1989 Loma Prieta earthquake, based on the Beroza (1991) and Wald et al. (1991) source models. For magnitude 7.8 ruptures on the northern San Andreas fault, they used a series of source models: first they used a source model by Song et al. (2008) inferred from the 1906 earthquake; then they modified the Song source model “to overcome limitations of the data available”; and finally they generated a random slip distribution for comparison.

The ground motions in this thesis are from the modified Song source model, generated by Brad Aagaard. For the same source model, there are three hypocenter locations: the inferred 1906 location, due west of San Francisco (bilateral rupture); a hypothetical location north of San Francisco, near Bodega Bay (unilateral rupture to the south); and a second hypothetical location south of San Francisco, near San Juan Bautista (unilateral rupture to the north). Aagaard et al. (2008b) considered several slip distributions and hypocenter locations to “assess the variability in the ground motions and distributions of shaking” in the various scenario earthquakes.

Table 3.1 lists the simulated earthquakes from the Aagaard et al. (2008a,b) studies that are used in this thesis, and Figure 3.1 maps the faults. Note that the 1906-like simulations are magnitude 7.8 whereas the 1906 earthquake was magnitude 7.9. Figures 3.2 and 3.3 show the long-period peak ground displacements ( $\text{PGD}_{\text{lp}}$ ) and peak ground velocities ( $\text{PGV}_{\text{lp}}$ ) for the five simulations. In this thesis, I measure the  $\text{PGD}_{\text{lp}}$  and  $\text{PGV}_{\text{lp}}$  as the largest vector amplitude of the two horizontal, north-south and east-west, components.

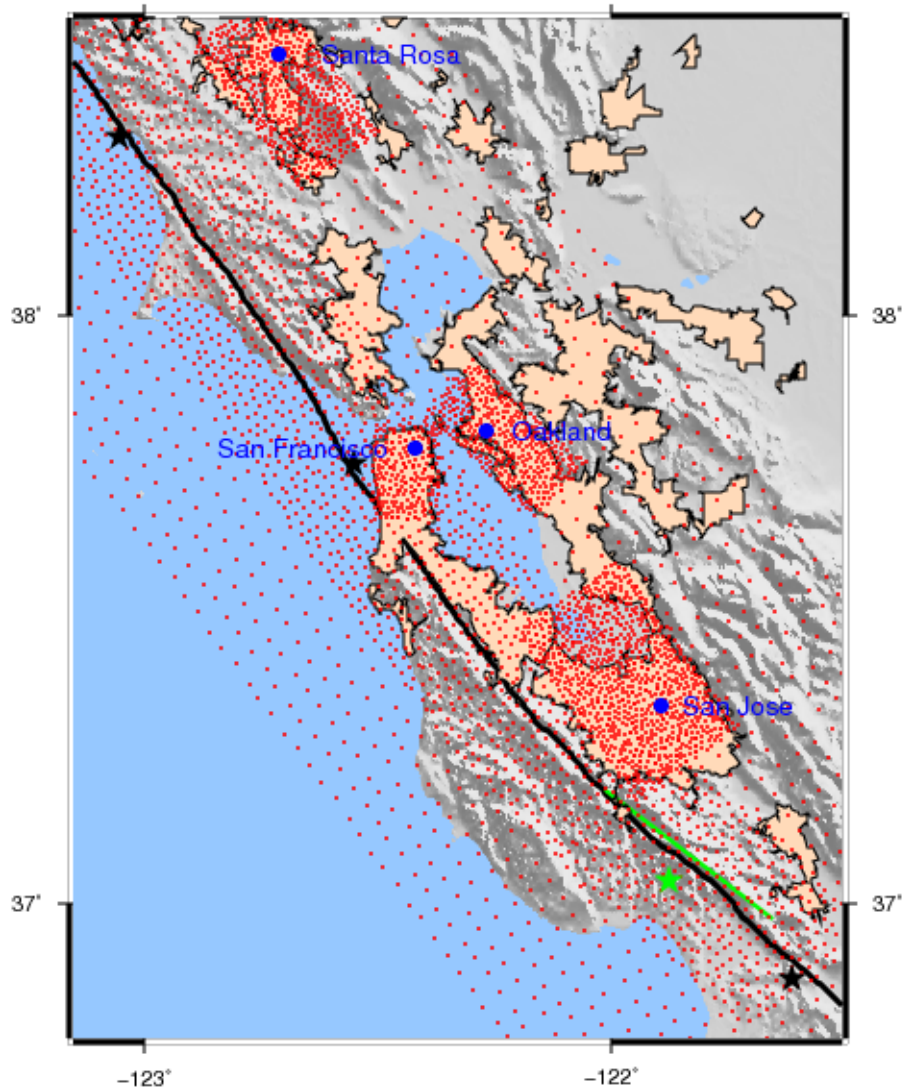


Figure 3.1: The simulation domain in Aagaard et al. (2008a,b) covers the San Francisco Bay area. Red dots locate the 4945 sites in the domain. Beige areas are the urban areas (as defined by the 2000 census). Blue dots locate major cities in the area that have simulation sites on a finer grid. The black line locates the San Andreas fault, and black stars locate the three hypocenters considered in the Aagaard et al. simulations. The green line represents the fault segment on which the Loma Prieta earthquake ruptured, and the green star locates its hypocenter.

<i>Fault name</i>	<i>Magnitude</i>	<i>Source model</i>	<i>Hypocenter location</i>
Loma Prieta	6.9	Beroza	1989 Loma Prieta
Loma Prieta	6.9	Wald et al.	1989 Loma Prieta
Northern San Andreas	7.8	modified Song	north of San Francisco
Northern San Andreas	7.8	modified Song	south of San Francisco
Northern San Andreas	7.8	modified Song	1906 San Francisco

Table 3.1: This table lists the five simulations used in this thesis generated by Aagaard et al. (2008a,b).

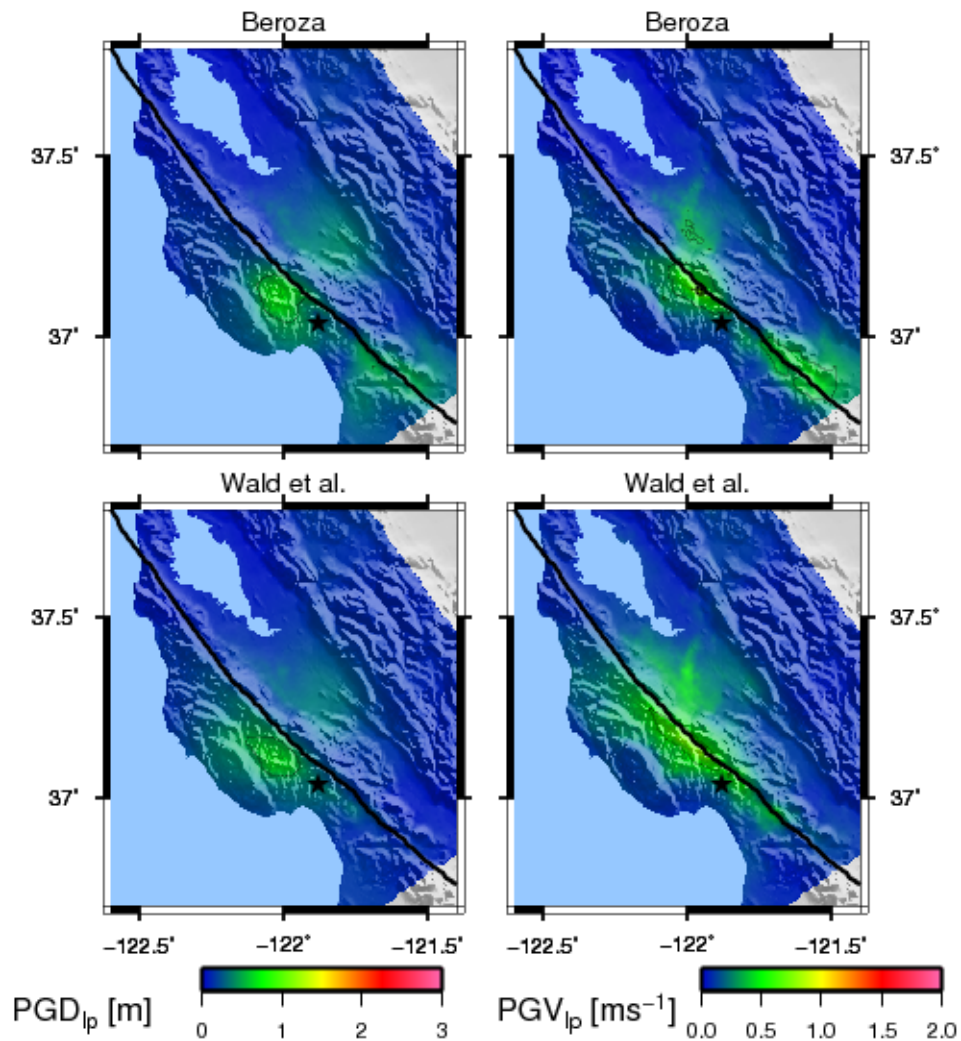


Figure 3.2: Aagaard et al. (2008a) generated ground motions from two source models of the Loma Prieta earthquake: Beroza (top maps) and Wald and others (bottom maps). The largest PGD<sub>lp</sub> are approximately 0.7 m, and the largest PGV<sub>lp</sub> are approximately 1.0 m/s. Compared to the magnitude 7.8 simulations, the Loma Prieta earthquake is a small event.

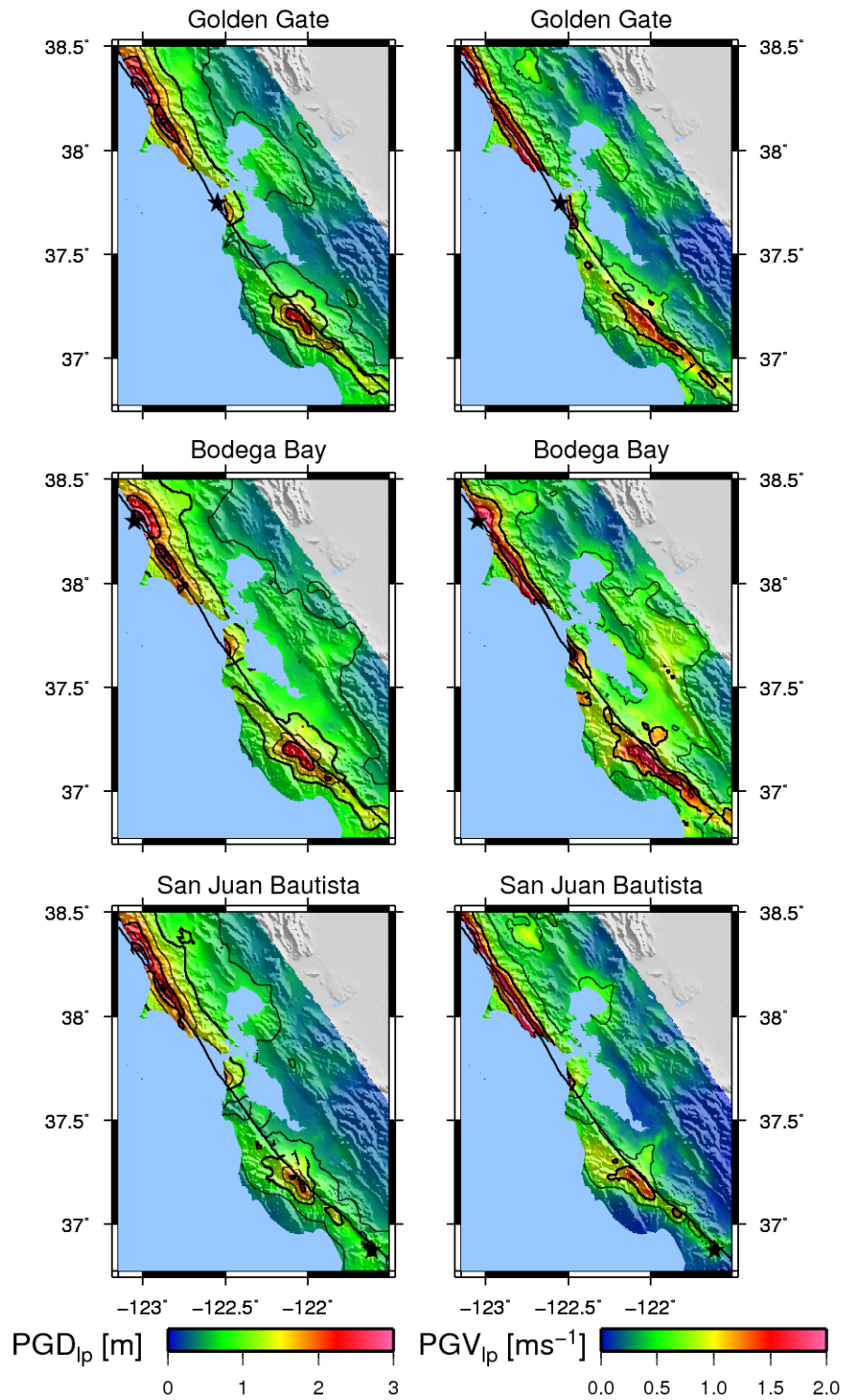


Figure 3.3: Aagaard et al. (2008b) used the same slip distribution (inferred from the 1906 event) and three hypocenter locations to simulate three magnitude 7.8 earthquakes on the northern San Andreas fault. All three simulations have large near-source directivity pulses.

## 3.2 Building Responses in Loma Prieta versus 1906-Like Simulations

The simulated building responses to the Loma Prieta ground motions are consistent with the experience of that earthquake. Figure 3.4 maps the peak inter-story drift ratios (IDRs) developed in the twenty-story building models and compares them to the urban areas south and east of San Francisco. The areas of largest building response are in the Santa Cruz mountains, and there are some mildly inelastic responses (colored green) in the urban areas near San Jose. These simulations predict no significant peak IDR from twenty-story steel MRF buildings in urban areas. The Beroza model causes a larger area of inelastic building responses than does the Wald et al. model, and the Beroza model induces large responses immediately northwest of the hypocenter. Figure 3.5 graphs the twenty-story building responses as a function of  $PGV_{1p}$ . There seems to be no systematic difference between the responses to ground motions from the two source models, even though the models predict different geographic patterns of response.

The 1989 magnitude 6.9 Loma Prieta earthquake is literally and figuratively on a different order of magnitude than the 1906 magnitude 7.9 San Francisco earthquake. Comparing the damage experienced in each earthquake is not a straightforward exercise: the building stocks in the San Francisco urban areas were significantly different in those years. Nonetheless, comparing the extent of damage in the two earthquakes is instructive. Most earthquake engineers today are familiar with the aftermath of the Loma Prieta earthquake, so that experience serves as a point of reference. If a 1906-like earthquake struck the San Francisco Bay area today, steel MRF buildings would be significantly damaged and possibly collapse. Compare the building responses in Figure 3.4 (Loma Prieta scenario) and Figure 3.8 (1906-like simulations). Tall steel MRF buildings in existing urban areas have significantly larger peak IDR in the 1906-like simulations than in the Loma Prieta scenario.

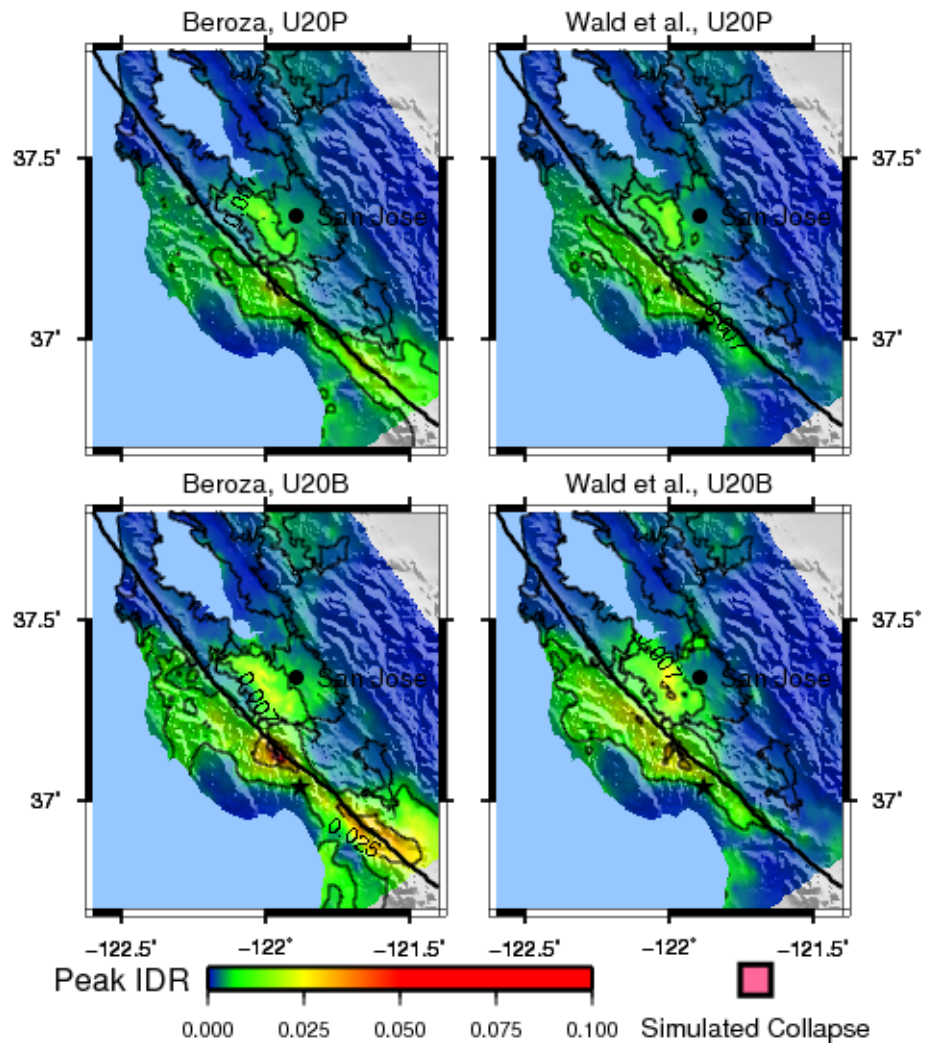


Figure 3.4: The twenty-story, more flexible building responses are similar for ground motions from the Beroza (maps on left) and Wald et al. (maps on right) source models. Urban areas and the city of San Jose are located. Existing steel MRF buildings in the San Jose area may have experienced inelastic building response and specifically some fractured welds, according to this simulation.

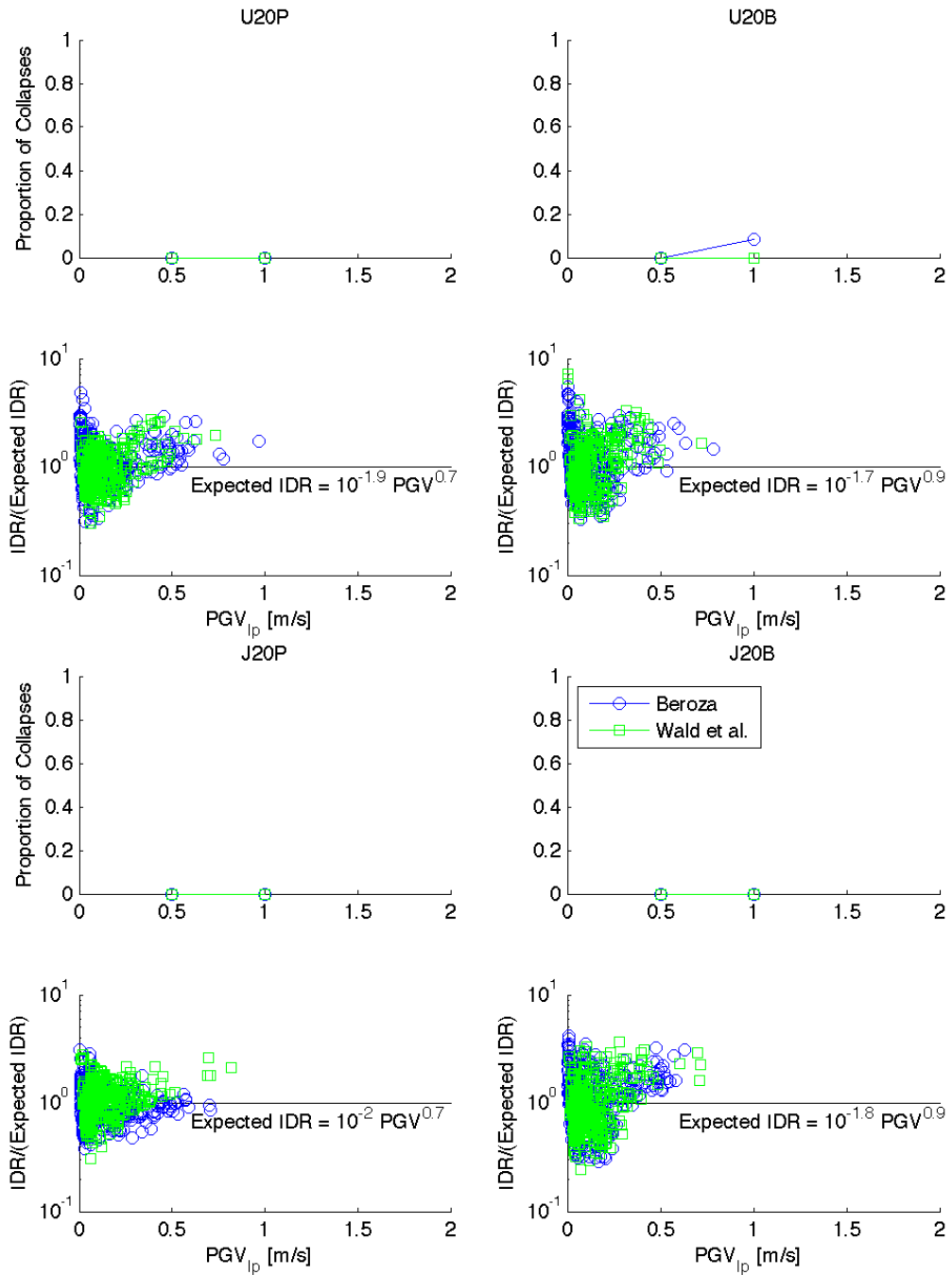


Figure 3.5: The twenty-story steel MRF building responses are not noticeably different for ground motions generated by the Beroza (1991) and Wald et al. (1991) source models of the 1989 Loma Prieta earthquake. In terms of building response as a function of  $\text{PGV}_{ip}$ , there is no reason to prefer one source model over the other.

### 3.3 Stiffer versus More Flexible Building Responses

The three magnitude 7.8 earthquakes provide sufficient data to compare the responses of the stiffer, higher-strength models (J20P) to the more flexible, lower-strength models (U20P). Figure 3.6 maps the peak IDRs of these two types of twenty-story buildings for the three simulations. The models show similar patterns of inelastic and collapse responses. The areal extent of inelastic responses appears larger, and the severity of the responses appears greater, for the more flexible, lower-strength model (U20P) compared to the stiffer, higher-strength model (J20P). Tables 3.2 and 3.3 verify these observations. For the urban area as a whole, and for almost all major cities individually, the more flexible, lower-strength model (U20P) collapses on greater percentages of urbanized areas compared to the stiffer, higher-strength model (J20P), for all three magnitude 7.8 simulations. The same statement could be made using exceedance of life safety (peak IDR greater than 0.025) as the response in place of collapse, with one exception: in the Bodega Bay simulation the stiffer, higher-strength model (J20P) response exceeds life safety on 1.6% of the Oakland sub-domain compared to 0.20% for the more flexible, lower-strength model (U20P).

Figure 3.7 directly compares the responses of the stiffer, higher-strength (J20P) and more flexible, lower-strength (U20P) buildings for each site in the three magnitude 7.8 simulations. The top graph reports the proportion of sites with a simulated building collapse. For all  $PGV_{1ps}$ , the more flexible, lower-strength (U20P) building collapses on a greater proportion of sites than does the stiffer, higher-strength (J20P) building. The bottom graph compares the ratio of the stiffer, higher-strength (J20P) building peak IDR to the more flexible, lower-strength (U20P) building peak IDR, assuming both models remain standing. For sites with  $PGV_{1ps}$  less than 1.5 m/s, this ratio is approximately 0.3–1.5. For sites with  $PGV_{1ps}$  greater than 1.5 m/s, it is approximately 0.7. For all  $PGV_{1ps}$ , the median ratio of J20P peak IDR to U20P peak IDR is 0.75. Thus, the more flexible, lower-strength building is more likely to collapse than the stiffer, higher-strength building, and the peak IDR of the more flexible, lower-strength building is approximately 1.3 times that of the stiffer, higher-

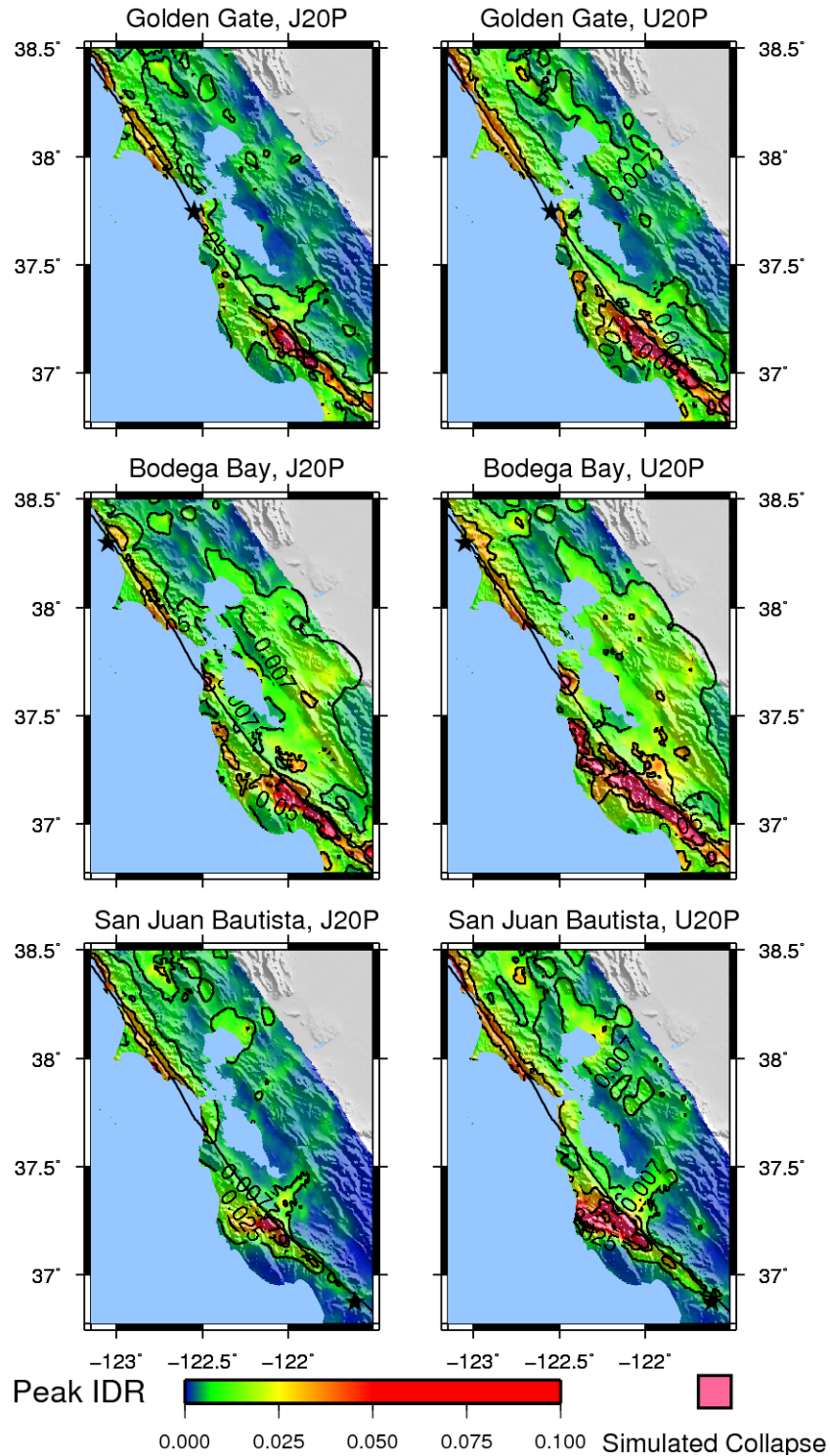


Figure 3.6: In terms of areal extent, there is some difference between the responses of the J20 models (maps on left) and the U20 models (maps on right). Compare the building responses at sites east of San Francisco Bay, for example: the U20 responses tend to be larger than the corresponding J20 responses.

Areas within the Entire Urban Outline [%] that Exceed a Peak IDR of 0.025				
	<i>J20B</i>	<i>J20P</i>	<i>U20B</i>	<i>U20P</i>
<i>1989 Loma Prieta</i>	0.079	0	0.40	0
<i>M 7.8 Bodega Bay</i>	36	4.6	54	10.
<i>1906 San Francisco</i>	9.3	0.99	15	3.1
<i>M 7.8 San Juan Bautista</i>	11	0.95	17	2.4
Areas within Oakland Sub-Domain [%] that Exceed a Peak IDR of 0.025				
<i>1989 Loma Prieta</i>	0	0	0	0
<i>M 7.8 Bodega Bay</i>	18	1.6	48	0.20
<i>1906 San Francisco</i>	0	0	0	0
<i>M 7.8 San Juan Bautista</i>	0	0	0	0
Areas within San Francisco Sub-Domain [%] that Exceed a Peak IDR of 0.025				
<i>1989 Loma Prieta</i>	0	0	0	0
<i>M 7.8 Bodega Bay</i>	48	18	69	35
<i>1906 San Francisco</i>	39	12	49	18
<i>M 7.8 San Juan Bautista</i>	63	6.8	92	13
Areas within San Jose Sub-Domain [%] that Exceed a Peak IDR of 0.025				
<i>1989 Loma Prieta</i>	0.20	0	1.7	0
<i>M 7.8 Bodega Bay</i>	64	11	83	26
<i>1906 San Francisco</i>	14	0.018	18	3.8
<i>M 7.8 San Juan Bautista</i>	11	0.51	14	1.6
Areas within Santa Rosa Sub-Domain [%] that Exceed a Peak IDR of 0.025				
<i>1989 Loma Prieta</i>	0	0	0	0
<i>M 7.8 Bodega Bay</i>	18	0	38	3.1
<i>1906 San Francisco</i>	25	0	25	8.6
<i>M 7.8 San Juan Bautista</i>	38	5.7	27	11

Table 3.2: Depending on the earthquake and building type, the simulated building responses may exceed the FEMA 356 life safety level on a limited or broad portion of the urban area. The Bodega Bay scenario earthquake especially causes damage in large parts of the San Francisco Bay urban area. The entire urban area in the simulation domain is 3266 km<sup>2</sup>. Reproduced from Olsen et al. (2008) with authors' permission.

Areas within the Entire Urban Outline [%] with Simulated Collapse				
	<i>J20B</i>	<i>J20P</i>	<i>U20B</i>	<i>U20P</i>
<i>1989 Loma Prieta</i>	0	0	0	0
<i>M 7.8 Bodega Bay</i>	1.7	0.049	6.6	0.24
<i>1906 San Francisco</i>	0.29	0	0.67	0.00092
<i>M 7.8 San Juan Bautista</i>	0.092	0	0.42	0
Areas within Oakland Sub-Domain [%] with Simulated Collapse				
<i>1989 Loma Prieta</i>	0	0	0	0
<i>M 7.8 Bodega Bay</i>	0	0	0	0
<i>1906 San Francisco</i>	0	0	0	0
<i>M 7.8 San Juan Bautista</i>	0	0	0	0
Areas within San Francisco Sub-Domain [%] with Simulated Collapse				
<i>1989 Loma Prieta</i>	0	0	0	0
<i>M 7.8 Bodega Bay</i>	8.8	0.89	24	4.1
<i>1906 San Francisco</i>	0.11	0	1.7	0
<i>M 7.8 San Juan Bautista</i>	1.3	0	1.6	0
Areas within San Jose Sub-Domain [%] with Simulated Collapse				
<i>1989 Loma Prieta</i>	0	0	0	0
<i>M 7.8 Bodega Bay</i>	3.2	0	15	0.033
<i>1906 San Francisco</i>	0.031	0	0.97	0
<i>M 7.8 San Juan Bautista</i>	0	0	0.59	0
Areas within Santa Rosa Sub-Domain [%] with Simulated Collapse				
<i>1989 Loma Prieta</i>	0	0	0	0
<i>M 7.8 Bodega Bay</i>	0	0	4.0	0
<i>1906 San Francisco</i>	0	0	0	0
<i>M 7.8 San Juan Bautista</i>	0.069	0	0.069	0

Table 3.3: Steel MRF building models with brittle welds show simulated collapses on a greater area than models with perfect welds. The stiffer, higher-strength models collapse on a greater area than do the more flexible, lower-strength models. The entire urban area in the simulation domain is 3266 km<sup>2</sup>. Reproduced from Olsen et al. (2008) with authors' permission.

strength building if both buildings remain standing.

These simulations also suggest that the near-source factors adopted in the 1997 Uniform Building Code (UBC) reduce the response of twenty-story steel moment frames in strong ground motions. Section 2.1.2 describes the near-source factors and the extent to which the building model designed to the 1992 Japanese Building Code (J20P) satisfies the 1997 UBC. The J20P model does not satisfy the 1997 UBC for all sites in the Aagaard et al. (2008a,b) simulation domain; specifically, the J20P model would not satisfy the 1997 UBC at sites within 5 km of the northern San Andreas. These sites would roughly correspond to the largest peak ground velocities in Figure 3.7. Disregarding the building responses in ground motions with long-period peak ground velocities greater than 1.5 m/s, the response of the J20P model is generally smaller than that of the U20P model. I infer that steel moment frame designs that satisfy the 1997 UBC at all sites would also have smaller responses than an equivalent design satisfying only the 1994 UBC, although the simulations in this thesis do not directly support this claim. The next section shows, however, that fixing brittle welds reduces building response more than designing a stiffer and stronger building.

### **3.4 Responses of Buildings with Non-Fracturing versus Fracture-Prone Welds**

The magnitude 7.8 simulations also provide data to compare the responses of models with sound (or perfect, P) welds to those with fracture-prone (or brittle, B) welds. Figure 3.8 maps the responses of models with perfect and brittle welds in the three magnitude 7.8 simulations. The area of inelastic response (colored green to pink) appears similar for the models with perfect and brittle welds. However, within the areas with inelastic response, the response is much larger for the models with brittle welds, and there are more collapses of models with brittle welds. Tables 3.2 and 3.3 confirm that the models with brittle welds have larger responses than those with

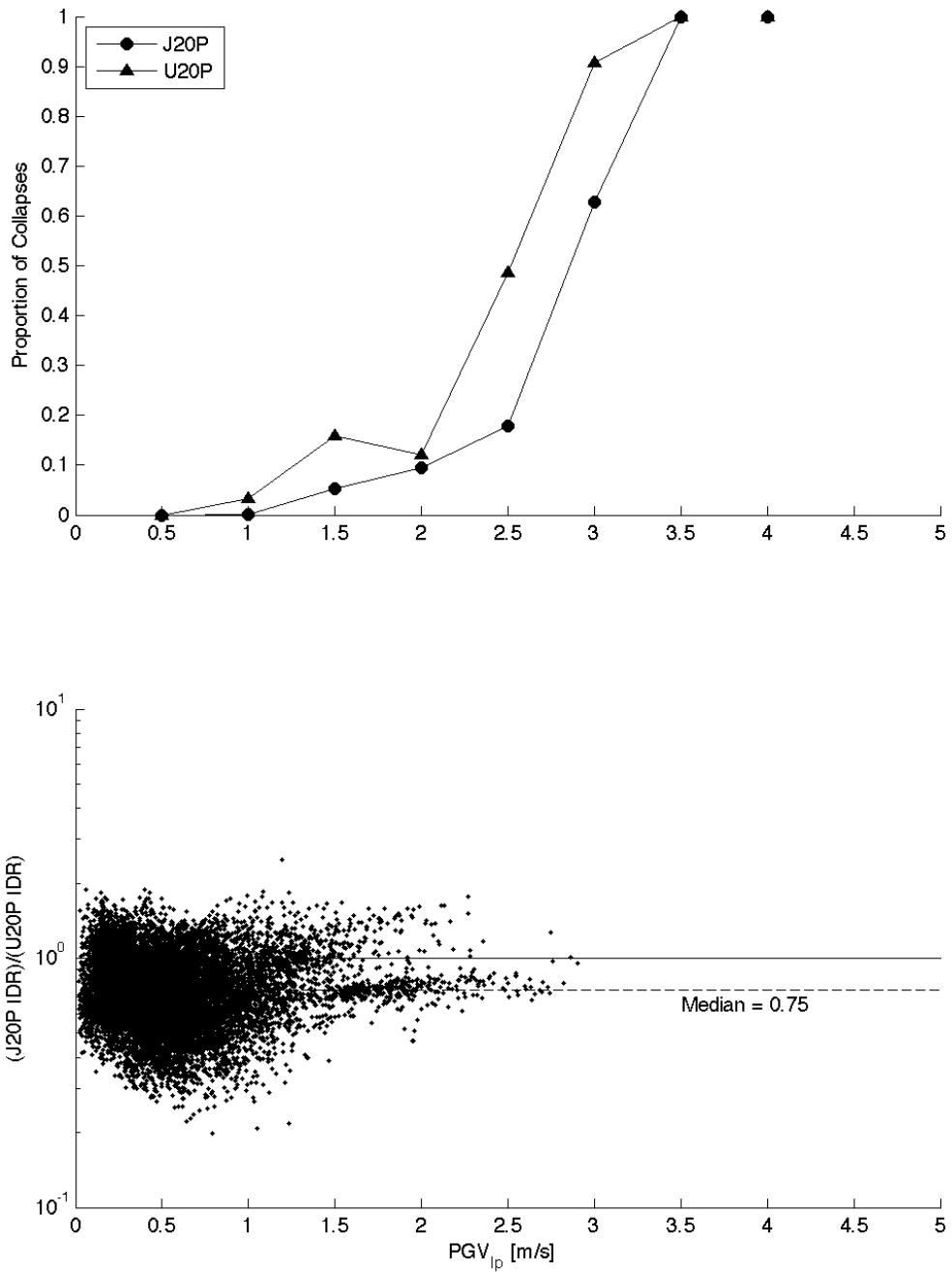


Figure 3.7: This figure compares the responses of J20P and U20P models at each site in the three magnitude 7.8 simulations. For the same  $PGV_{ip}$ , the U20 model is more likely to collapse while the J20 model stands. If both buildings remain standing at a site, the peak IDR in the J20 model is most likely to be 0.75 times the peak IDR in the U20 model.

perfect welds in the same simulations. For both the more flexible, lower-strength and stiffer, higher-strength models, the response of the brittle weld models exceeds life safety on an area 2–20 times that of perfect weld models. Similarly, the model with brittle welds collapses on an area 6–30 times that of the models with perfect welds.

Figure 3.9 directly compares the responses of the models with each weld state at each site in the magnitude 7.8 simulations. Similar to Figure 3.7, the top graph of Figure 3.9 reports the proportion of sites with a simulated building collapse. For all  $PGV_{IP,S}$ , the brittle weld model collapses on a notably greater proportion of sites than does the perfect weld model. The bottom graph of Figure 3.9 compares the ratio of the brittle weld model peak IDR to the perfect weld model peak IDR, assuming both models remain standing at the site. Most of these ratios are 0.5 to 5, with a median of 1.7. For the smallest  $PGV_{IP,S}$ , this ratio is 1, implying that the building response remains elastic. In the elastic region, the responses of the two models are the same because the brittle welds remain sound. In the inelastic region, however, the brittle welds significantly degrade the lateral load-resisting capacity of the models.

### 3.5 Effect of Rupture Propagation Direction

Rupture propagation on the northern San Andreas fault significantly affects the geographic pattern of building responses. Both Figures 3.6 and 3.8 demonstrate this effect. In the north-to-south rupture (Bodega Bay), the San Francisco peninsula and areas east of the Bay experience larger building responses than in the other two simulations. The 1906 bilateral rupture (Golden Gate) generally induces lower building responses than does the north-to-south rupture, and the largest responses are limited to areas near the fault. The largest building responses to the south-to-north rupture (San Juan Bautista) are also close to the fault, with a large area of elastic response southeast of San Jose. Tables 3.2 and 3.3 show that the Bodega Bay scenario earthquake is the most damaging of the three simulations for the urban area as a whole. However, the cities of San Francisco and Santa Rosa experience large areas of life threatening responses in the San Juan Bautista scenario earthquake. On its

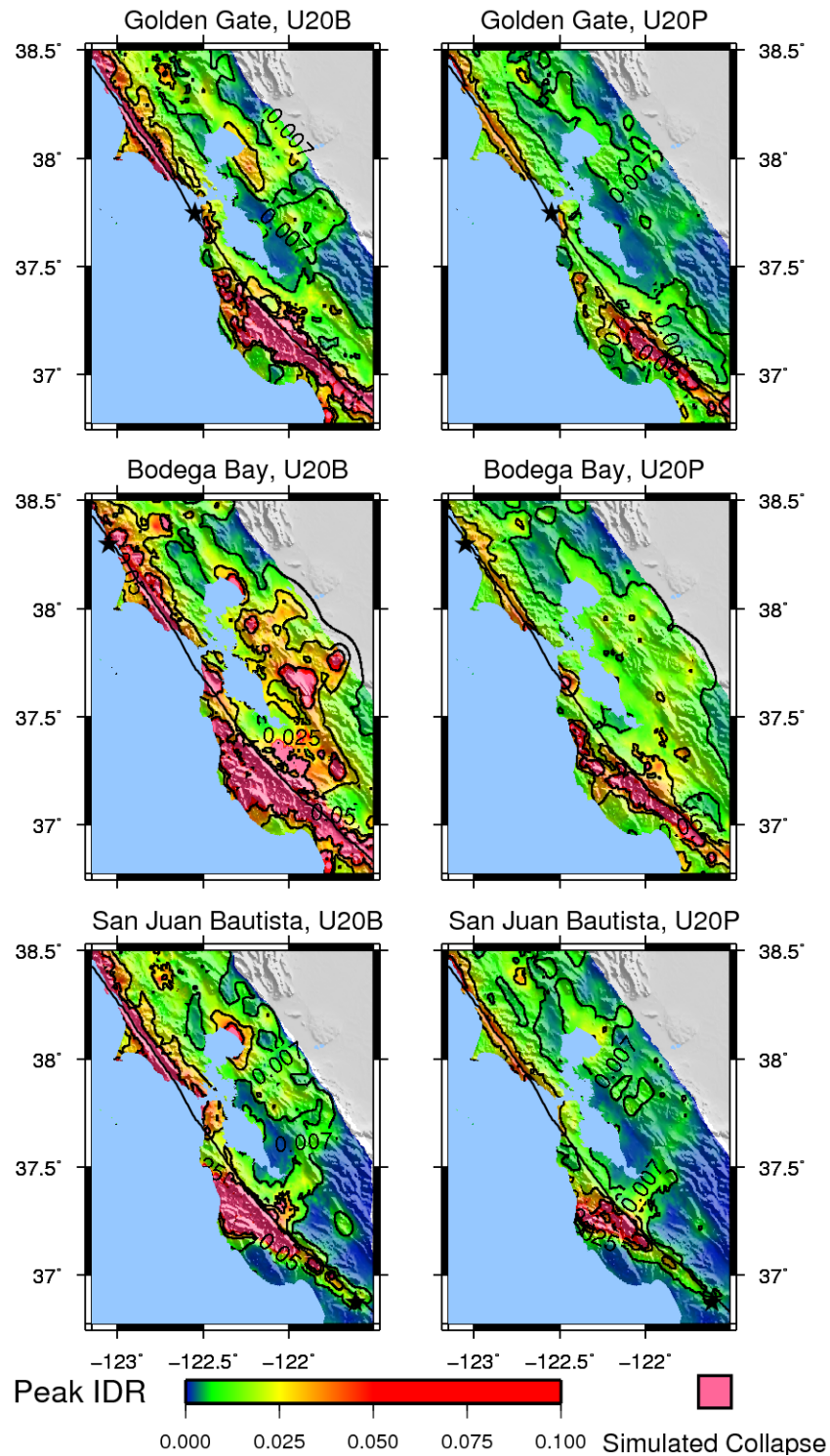


Figure 3.8: The weld state (that is, perfect or brittle) significantly affects building responses. Compare the extent of large peak IDR (peak IDR greater than 0.025, colored yellow to pink) for models with brittle welds (maps on left) and models with perfect welds (maps on right). In the city of San Francisco, for example, the perfect weld peak IDR is generally 0.007–0.025 while the brittle weld peak IDR is generally 0.007–collapse.

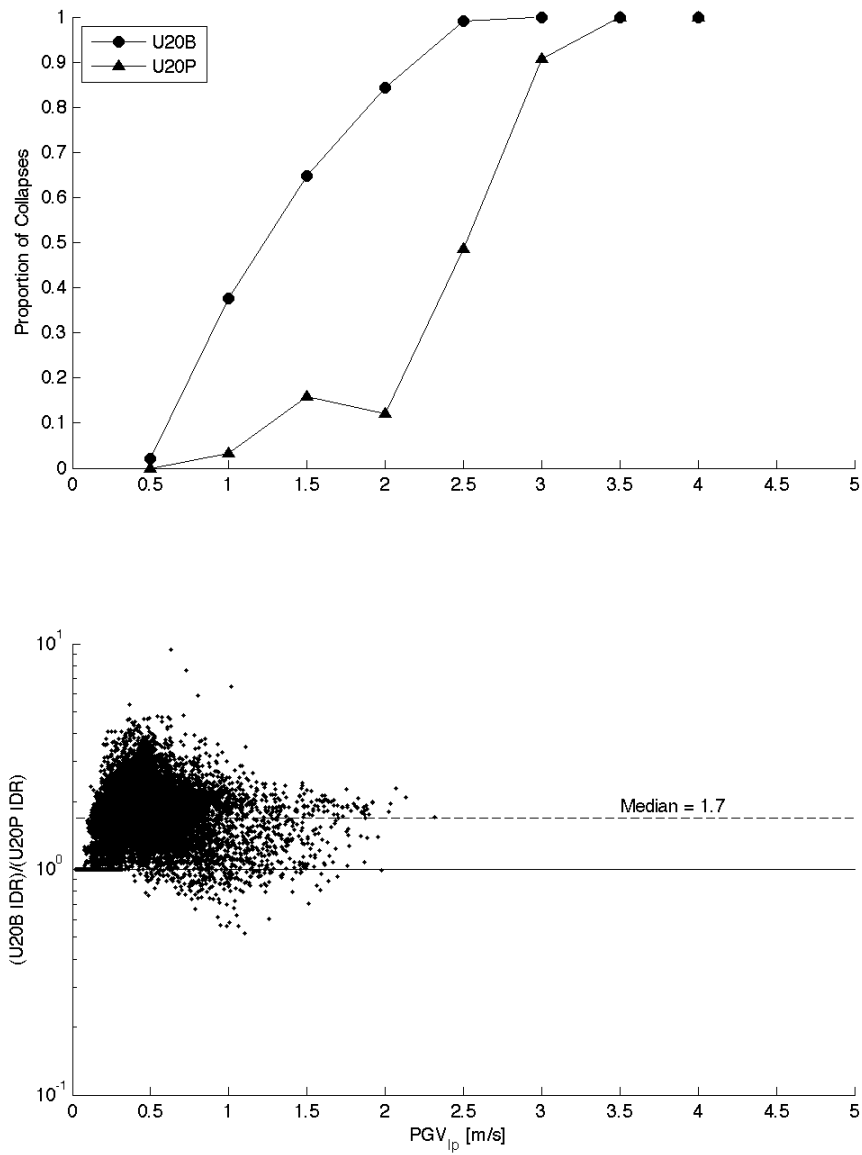


Figure 3.9: This figure compares the response of models with brittle and perfect welds directly at each site of the three magnitude 7.8 earthquakes. The brittle weld model is much more likely to collapse than the perfect weld model. Consider  $PGV_{IP}$  of approximately 2 m/s: on 80% of those sites the brittle weld model collapses compared to 10% for the perfect weld model. If both models stand at a site, the peak IDR in the brittle weld model is likely 1.7 times the peak IDR in the perfect weld model.

own, the 1906 scenario causes significantly large steel MRF responses in the urban areas around the San Francisco Bay, even though the responses tend to be smaller in comparison to the two earthquakes with hypothetical hypocenters.